# Carbon contamination and oxidation of Au surfaces under extreme ultraviolet radiation: An x-ray photoelectron spectroscopy study

Al-Montaser Bellah Al-Ajlony,[a)] Aloke Kanjilal, Sivanandan S. Harilal, and Ahmed Hassanein
*Center for Materials Under Extreme Environment, School of Nuclear Engineering, Purdue University, West Lafayette, Indiana 47907*

Extreme ultraviolet (EUV) radiation-induced carbon contamination and oxidation of Au surfaces were investigated using x-ray photoelectron spectroscopy (XPS). The Au sample was irradiated by EUV radiation at 13.5 nm for 9 h, while a series of XPS spectra were recorded for monitoring chemical modification during EUV exposure. XPS analysis showed that total carbon contamination (C 1$s$ peak) at the surface was increased by ∼14% after 9 h of EUV exposure, while the C–H component played a dominant role within the first 60 min of EUV irradiation, giving a sharp rise of the corresponding C 1$s$ peak intensity, followed by a slow and linear increase in intensity of the C–C bonds. The later one represents an accumulation of carbon due to the EUV-assisted dissociation of residual hydrocarbons on Au surface. Oxide state of Au was also noticed to be formed during EUV irradiation, and was found to increase continuously before reaching its maximum followed by a progressive decay. The role of water dissociation in the presence of EUV radiation was discussed and correlated with Au oxidation phenomenon. © *2012 American Vacuum Society*. [http://dx.doi.org/10.1116/1.4737160]

## I. INTRODUCTION

In a vacuum chamber, carbon atoms are generally deposited onto a solid surface when residual hydrocarbons encounter a dissociation process during interaction with an ionizing radiation such as x-ray or extreme ultraviolet (EUV) light.[1] The carbon atoms can then accumulate at the optics surfaces, which in turn change optical characteristics and reduce the reflectivity[1] of mirrors. For example, EUV light-induced carbon contamination of Au grazing incidence optics in synchrotron beam lines is one of the major reasons for reduced reflectivity. This problem has been observed and investigated several decades ago, considering its cost and time consumption implications to synchrotron radiation beam quality and stability.[2] In order to retrieve the original optical characteristics of the contaminated optics, several cleaning procedures have been suggested so far.[3–5] This is also true for the development of novel hybrid Au-multilayer-Au in-line EUV optical polarizers where Au is used as a reflector with polarizing multilayer.[6]

Currently, EUV light sources emitting at 13.5 nm are being considered as the wavelength of next generation lithography, which are capable of producing electronic devices with feature sizes of 16 nm and beyond.[7,8] The extreme ultraviolet lithography (EUVL) system consists of high-vacuum system, light source, and the optics. Such a combination represents the exact recipe for EUV-induced carbon contamination of the optics. In fact, the EUVL system is very sensitive to the reduction in extreme ultraviolet reflectivity (EUVR), which can only be tolerated up to a few percent over the entire lifetime of the optics (estimated to be 30 000 working hours).[9] Typically, mirrors for EUVL systems are prepared by depositing alternating layers of Si and Mo.[10] Such multilayer mirrors (MLMs) are able to reflect electromagnetic radiation at a wavelength of 13.5 nm (92 eV). However, for the sake of better chemical stability of the top Si surface, a thin Ru capping layer has been suggested on top of a Si/Mo MLM.[11] Although Ru is considered the material of choice to protect Si/Mo layers because of its optical properties (high transmission coefficient at 13.5 nm) and high chemical resistance in corrosive environments,[12] EUV-induced carbon contamination is one of the major problems that reduces the duty life of MLMs,[1,13,14] and ultimately increases the operating cost of the EUVL process. Using different surface treatment with ions or even during the growth of a layer, the lifetime of a standard Mo/Si MLM system can, however, reach thousands of hours.[15]

Extensive research has been devoted worldwide to understand and to mitigate the formation of a carbonaceous layer on Ru surface during EUV exposure.[1,14] However, in-depth understanding of the EUV-induced carbon deposition process on Ru surfaces is hindered by the overlapping of the C 1$s$ and Ru 3$d$ lines in x-ray photoelectron spectroscopy (XPS),[16] which is the most common tool for observing and understanding the surface chemical properties. Similar to XPS, spectral analysis of Ru/C surfaces is also challenging for Auger electron spectroscopy (AES)[17] due to the same overlapping phenomenon. As a result, important details about the chemical nature of accumulated carbon are limited. In order to reveal insights regarding carbon deposition process during EUV exposure via dissociation of residual hydrocarbons, it is therefore important to choose a material that is not only compatible with EUV radiation, but also free of any core level bands near the binding energy (BE) region of C 1$s$ (285.4 eV).[18] Based on these concepts, we have chosen Au film as the model candidate to analyze EUV-induced carbon deposition mechanism using XPS. Moreover, Au surface is inert for most of the adsorbed molecules at room

---

a)Electronic mail: aalajlon@purdue.edu

temperature and therefore allows us to study the behavior of adsorbed (physisorbed) hydrocarbons during EUV exposure without having any dominant chemical reaction with reactive molecules such as water—opposite to the one observed in the case of Ru.[16] Although the accumulation of carbon on Au does not serve as a quantitative indicator for the growth of carbon on Ru surface, it might be useful to understand the physics of hydrocarbons dissociation under EUV irradiation. Moreover, the chemical states of accumulated carbon on Au and their temporal evolution during the EUV exposure will also be useful for developing an EUV optical polarizer.

The main purpose of this investigation is to provide information about the mechanisms of carbon contamination and to shed light on the chemical states of accumulated carbon and their temporal evolution. In particular, we aimed to show the hydrocarbons adsorption dynamics on the Au surface and its gradual transformation into graphite during the course of EUV irradiation. We also show the effect of EUV radiation on Au in the presence of water molecules and compare the results with the oxidation reaction of Au in ozone atmosphere under UV exposure.[19,20]

In this study we did not inject any hydrocarbons in our mildly baked ultrahigh vacuum (UHV) chamber. We relied on the residual hydrocarbons and water molecules that exist naturally in any vacuum system. Also, we maintained a high-vacuum condition to replicate the vacuum condition of EUVL systems.[21]

## II. EXPERIMENTAL DETAILS

The experiments have been performed at the surface characterization laboratory IMPACT[22,23] of the Center for Materials Under Extreme Environment at Purdue University. A 99.9% pure, 1 $\mu$m thick Au layer deposited on a quartz substrate (diameter $\sim$15 mm) was initially sputter cleaned by 2 keV $Ar^+$ for about 90 min (beam current $\sim$0.5 $\mu$A) using Nonsequitur Technologies Inc. ion source in a mildly baked UHV chamber (base pressure $\sim$5 $\times$ $10^{-9}$ Torr). The UHV chamber is equipped with a number of *in situ* diagnostic tools for surface analysis, such as XPS, AES, low energy ion scattering spectroscopy, EUV photoelectron spectroscopy, and EUVR.[22,23] For XPS analysis, the Au surface was excited using Al $K\alpha$ radiation ($h\nu = 1486.6$ eV), while the photoelectrons emitted at 45° from the target surface were analyzed employing a hemispherical electrostatic energy analyzer (Phoibos 100 from SPECS Gmbh). Calibration of BE scale with respect to the measured kinetic energy was made using the Au $4f_{7/2}$ line at 84.00 eV.[18]

The sample was exposed to radiation from a Phoenix EUV source[22,24] that emits light in the range of 12.5–15 nm with maximum peak at $\sim$13.5 nm.[24] The estimated EUV beam power reaching the target surface is $\sim$0.3 $\mu$W,[22,24] while the power of the 13.5 nm wavelength of light (within 2% bandwidth) is $\sim$0.1 $\mu$W.[22,24] The EUV beam spot size on the Au surface was measured to be $\sim$7 mm. During sputter cleaning of the Au surface, the chamber pressure was at $\sim$2.0 $\times$ $10^{-8}$ Torr. As the EUV source is mounted in a separate vacuum chamber with a differential pumping arrange-

ment, the working pressure of the experimental chamber during EUV irradiation was $\sim$2.0 $\times$ $10^{-8}$ Torr. The chamber atmosphere was analyzed with a residual gas analyzer. It shows the presence of water molecules with a partial pressure of $\sim$5.5 $\times$ $10^{-9}$ Torr, and different background hydrocarbons such as methane, acetone, ethyl alcohol, methyl alcohol, benzene, toluene, methane, etc.

## III. RESULTS AND DISCUSSION

The sputter cleaned Au surface was irradiated by EUV light for 9 h, while the XPS spectra were recorded at different time intervals during EUV exposure to account for surface chemical modification. In this investigation, we focused on O 1*s*, C 1*s*, and Au 4*f* regions. Figure 1 displays a typical XPS spectrum recorded after sputter cleaning of Au. The prominent core levels of Au, O, and C are marked accordingly.

The high resolution scan of the C 1*s* core peak is displayed in Fig. 2 after 10 min and 9 h of EUV exposure. As a major indication of EUV-induced carbon contamination, total carbon peak area intensity (at C 1*s* region) was found to be increased by $\sim$14% after 9 h of EUV irradiation. Careful analysis reveals that the C 1*s* region is composed of *four* different chemical states of carbon[25,26] (see Fig. 3): graphitic carbon or C–C bonding situated at 284.5 eV,[26] C–H at 285.4 eV,[26] and two oxide states related to C=O in carbonyl and carboxyl groups situated at 286.4 and 287.6 eV, respectively.[25] Furthermore, the change in each chemical state of carbon has systematically been tracked with EUV radiation time and documented in Fig. 4.

As can be seen from Fig. 4, the relative peak (area) intensity of the C–H bonding has reached an equilibrium condition after a rapid increase in intensity in the first 60 min of EUV radiation. We should mention that the relative intensity (here and also in the following) signifies the ratio between the recorded data with EUV radiation and the one just after sputter cleaning. Also note that the Au surface was exposed
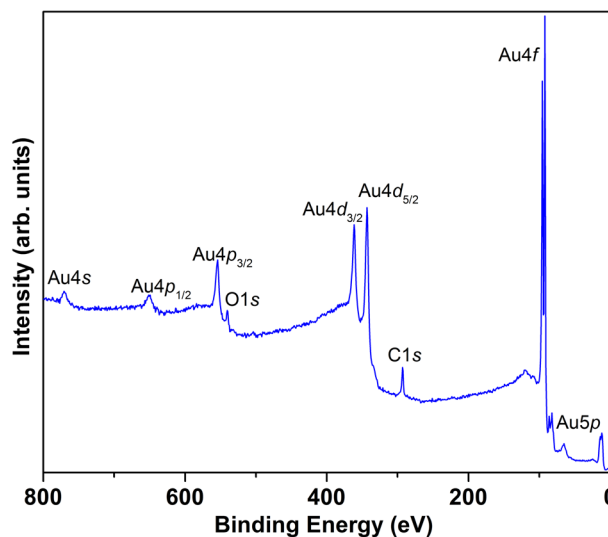


FIG. 1. (Color online) Typical XPS spectrum of Au after sputter cleaning, showing different core level peaks of Au such as Au 4*s*, Au 4*p*, Au 4*d*, Au 4*f*, and Au 5*p* along with O 1*s* and C 1*s* regions.
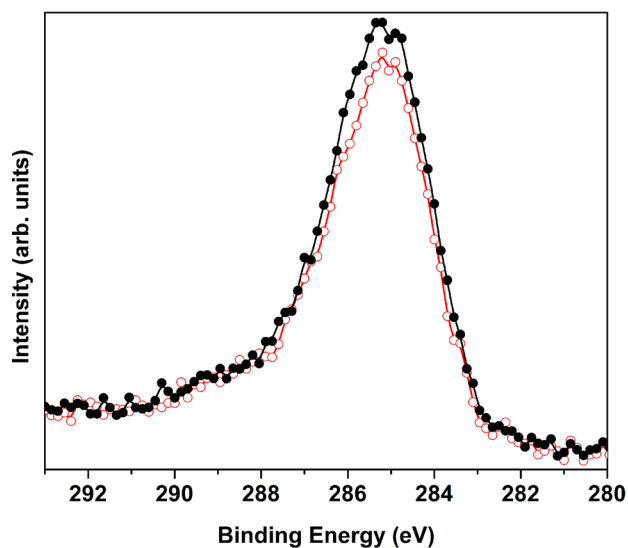
FIG. 2. (Color online) C 1*s* region of Au surface after EUV exposure for 10 min (open circles) and 540 min (closed circles).

to EUV radiation 30 min later after finishing the sputter cleaning process as the hydrocarbon adsorption is a slow process; it generally needs about 90 min to saturate at the sample surface in high-vacuum atmosphere.[16] The existence of C–H component confirms the adsorption of hydrocarbons on Au (see Fig. 3). On the other hand, the C–C peak intensity increases at a higher rate in the first 60 min of EUV radiation, though the growth rate is much lower than that of C–H (Fig. 4). After 60 min, the C–C intensity continued to increase linearly - however at a lower rate, until the end of our experimental run. Similar to intensity changes of C–H with time, a relatively fast increase in C–C peak intensity within 60 min of EUV exposure can also be explained in the
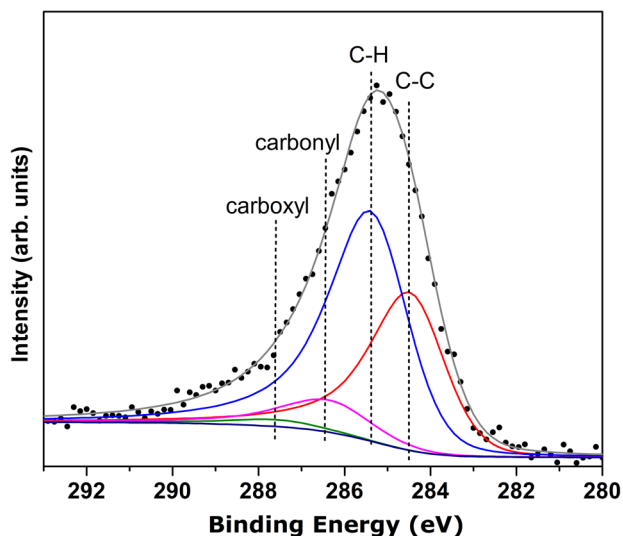


FIG. 3. (Color online) XPS spectrum of Au at C 1*s* region: Experimental data (dots) fitted with four components (thin lines) situated at 284.5 eV (C–C bonding), 285.4 eV (C–H bonding), and at 286.4 and 287.6 eV for carbonyl and carboxyl groups, respectively. The spectrum was recorded after 10 min of EUV exposure. The fitted curve is represented by a thick gray line, where four different peak positions of the fitting components are indicated by (dashed) vertical lines.
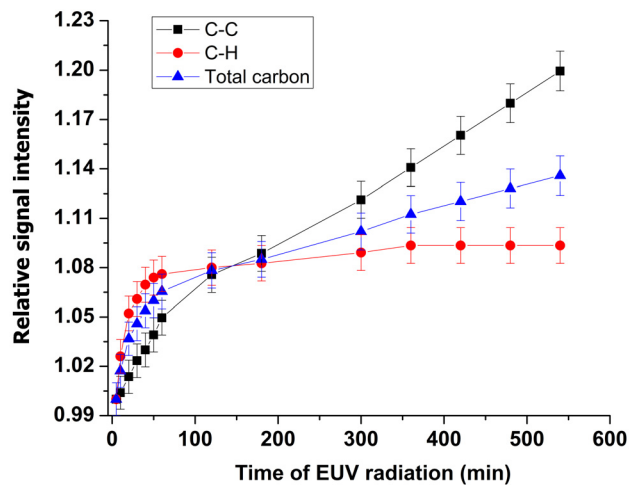


FIG. 4. (Color online) Using XPS spectra at the C 1*s* region, showing evolution of peak intensity of the fitting components C–C and C–H along with total carbon with EUV radiation time.

light of hydrocarbon adsorption, since the C–C bonds are the backbone of any hydrocarbon structure.

Since the number of C–C bonds in most of hydrocarbons is lower than the C–H bonds, one can expect lower carbon signal from C–C bonds than that of C–H of the adsorbed hydrocarbons. This is also in agreement with Fig. 3. The observed lower rate of increase in C–C peak intensity compared to C–H line in the first 60 min of EUV irradiation (Fig. 4) confirms superiority of hydrocarbon adsorption over carbon accumulation via dissociation of hydrocarbons.[1] Moreover, the linear increase in C–C peak intensity after 60 min can be discussed in the framework of accumulation of graphitic carbon due to EUV-assisted decomposition of the adsorbed hydrocarbons at the sample surface.[2,17] In fact, EUV-induced molecular dissociation depends on both the concentration of the adsorbed hydrocarbons on Au and the photon flux (EUV power density).[1] In this experiment, we have used a constant EUV power, whereas the adsorbed hydrocarbon concentration was found to be constant after 60 min of EUV irradiation (concluded from the C–H line). Hence, the linear behavior of carbon deposition is expected to be associated with EUV-induced dissociation of hydrocarbons. Our results, therefore, demonstrate that soon after complete hydrocarbon coverage on Au, accumulation rate of carbon via EUV-induced decomposition of adsorbed hydrocarbons exceeds the adsorption rate of hydrocarbons on Au, and thus contributes to total carbon deposition process (Fig. 4).

The oxide states of carbon related to C=O in carbonyl and carboxyl groups were found to be weak (Fig. 3), where the corresponding peak intensity fluctuates about the same value without any particular trend (not shown). The total carbon signal, therefore, represents nearly the sum of the peak area intensities of the C–C and C–H lines. In fact, sharp increase in intensity of total carbon within the first 60 min of EUV radiation (Fig. 4) seems to be controlled by the growth of C–H component, whereas the slow but linear increase is mainly associated with the C–C bonds concentration

evolution. Similar behavior of the accumulation of carbon has previously been observed also on the top of Au and Ru mirrors.[2,16] In general, we can conclude that adsorbed hydrocarbons on top of Au were continuously "enriched" with carbon atoms with increasing EUV irradiation time.

Along with carbon contamination, we also investigated oxidation of Au surface during EUV exposure by analyzing O 1s and Au 4f core lines. Figure 5 exhibits the O 1s and Au 4f regions after 10 and 120 min of EUV radiation. The Au 4f doublet pair, which represents the Au $4f_{5/2}$ and $4f_{7/2}$ states of pure Au (Au$^0$) situated at 84.0 and 87.7 eV, respectively,[18] was fitted with two peaks after background subtraction [Figs. 5(b) and 5(d)]. With increasing EUV irradiation time, a slight change in peak shape and intensity was detected. Using similar fitting constraints as in Fig. 5(b), the appearance of additional oxide states of the respective Au$^0$ doublet was noticed at the higher binding energy side at ~89.1 and 85.4 eV (Ref. 27) [Fig. 5(d)]. This is also consistent at the O 1s region [see Figs. 5(a) and 5(c)].

Figure 6 shows the temporal evolution of the relative peak area intensity for both pure and oxide states of Au. As apparent, the Au$^0$ peak intensity is decreased at higher rate in the first hour of EUV radiation, followed by a lower rate up to the end of experiment. Considering both these trends, total Au$^0$ peak intensity was found to be reduced by ~4% after 9 h of EUV irradiation. On the other hand, an evolution of oxide state of Au (Au–O) was found to be increased with EUV exposure until it reached its maximum within 200–300 min, which is followed by a progressive decrease in intensity up to the end of the experiment. In fact, surface oxidation of Au has also been confirmed by taking the ratio of the Au–O peak intensity to that of Au$^0$, which is also given in Fig. 6. As can be seen, the ratio exhibits a similar trend as found in Au–O evolution behavior. Clearly, the observed oxidation is associated with



FIG. 6. (Color online) From Au 4f region, time dependent change in Au$^0$ (left ordinate) and Au–O (right ordinate) peak intensities at the Au 4f region of the recorded XPS spectra with EUV exposure. The EUV exposure time dependent corresponding change in ratio of Au–O to Au$^0$ peak intensities is shown by using the extreme right ordinate.

EUV radiation since we did not find any oxide state before EUV exposure. Moreover, the decreasing behavior of Au$^0$ (see Fig. 6) is associated with the accumulation of carbon and/ or hydrocarbons, which as a result enhances inelastic scattering of photoelectrons from Au$^0$ when passing through surface carbonaceous layer.[17]

In order to understand further about Au oxidation, the O 1s region has also been analyzed. Initially, the recorded O 1s peak was fitted with two components, representing oxygen in two different chemical states, such as OH and H$_2$O peaking at 531.7 eV (Ref. 20) and 533.2 eV (Ref. 18), respectively [see Fig. 5(a)]. However, with increased EUV exposure, another peak situated at 530.1 eV (Refs. 20, 27, and 28) was found to be formed and evolved with time [Fig. 5(c)], confirming the oxidation process of Au under EUV exposure. The changes in H$_2$O and Au–O peak intensities in the O 1s region were also monitored as a function of EUV exposure time and given in Fig. 7. As discerned, the H$_2$O peak intensity was decreased dramatically in the first 2 h of EUV radiation, followed by gradual flattening in the remaining time. The
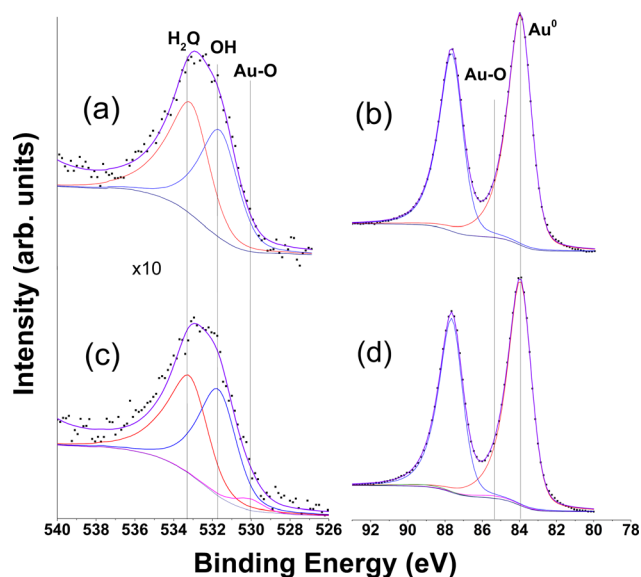


FIG. 5. (Color online) XPS spectra of Au, showing the O 1s (a) and Au 4f (b) regions after 10 min of EUV irradiation, and also the O 1s (c) and Au 4f (d) after 120 min of EUV irradiation. The O 1s spectra are multiplied by a factor of 10 for clarity, whereas vertical lines are used to project peak positions when fitting the recorded experimental data (dots).
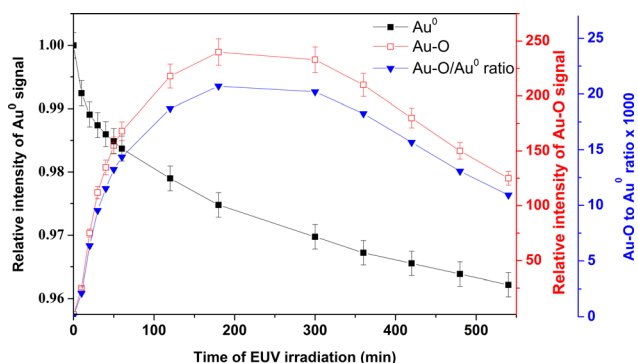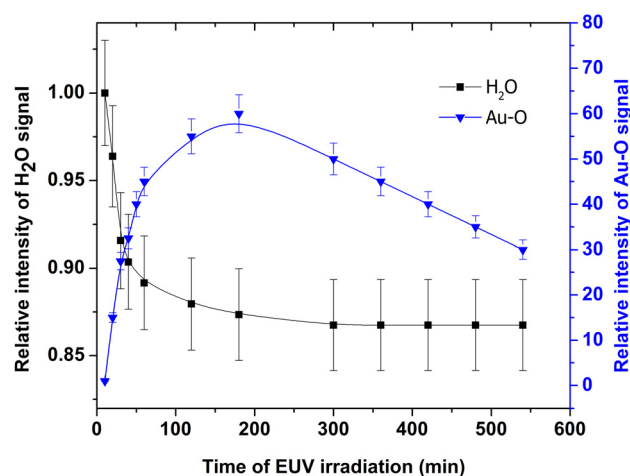


FIG. 7. (Color online) From O 1s region, the EUV exposure time dependent variation of H$_2$O (left ordinate) and Au–O (right ordinate) peak intensities, extracted by using a fitting procedure at the O 1s region of the recorded XPS spectra.

observed decrease of water content is most likely due to continuous dissociation of water molecules under EUV exposure.[16,29] As a result of water dissociation, the dissociated fragments, particularly free O atoms, are able to interact and oxidize Au atoms.[29] Hydrocarbon adsorption and its subsequent carbon deposition (see Fig. 4) are also responsible for the reduction of $H_2O$ surface concentration with time. In fact, binding energy of $H_2O$ molecules to metal surface is strongly influenced by the surface concentration of other contaminants such as O, N, C, etc. Generally, surface carbon weakens the adsorption energy of water molecules on metal surfaces.[29] Another reason for the observed water desorption is the partial surface oxidation of Au (Fig. 6) as the adsorption of water molecules on metal oxides has less binding energy compared with water adsorbed directly on pure metals.[29]

It has long been believed that the noble-metal Au is inert and has low affinity toward oxygen.[30] Recent results suggest that the missing row type reconstructed Au (110) surface is favorable for adsorbing atomic oxygen, where the chemisorption energy was evaluated to be ~0.35 eV.[30] Although dissociative adsorption of $O_2$ on Au in a vacuum chamber has not yet been observed by thermal desorption spectroscopy, this phenomenon is at present fueled by the catalyzing property of the Au nanoparticles (see Ref. 30, and references therein). In fact, it has been demonstrated theoretically that the molecular and dissociative adsorption of oxygen are controlled by the size of Au clusters.[31] Yoon *et al.*[31] have shown that the bonding mechanism involves charge transfer to oxygen from the Au cluster with a concomitant activation of the O–O bond to a superoxo state. Moreover, the anionic Au clusters with three or less atoms can initiate molecular adsorption, whereas dissociative adsorption of oxygen is expected in bigger clusters with corrugated structure.[31] The interaction of O with neutral and cationic Au clusters was, however, reported to be very weak,[32] and thus does not induce O–O bond activation.[31] On the other side, thermal dissociation, O-ion sputtering, microwave discharge, and use of reactive molecules like $NO_2$ can also form chemisorbed O species on Au (see Ref. 30, and references therein).

Several studies are also concerned with oxidation of Au in the presence of $O_3$[3] and UV light,[19,20,28] where the weakly bonded $O_3$ can be dissociated into $O_2$ and free O under UV radiation.[19] Since the dissociative adsorption of $O_2$ by Au at room temperature is thermodynamically not favorable,[30,32] it is clear that the oxidation of Au upon UV exposure in the presence of $O_3$ atmosphere is mainly driven by free O atoms. Based on $O_3$-UV oxidation phenomenon, we believe that Au in the present investigation is most probably oxidized by free oxygen atoms upon EUV-induced water dissociation,[1,29] where ion sputter cleaned rough Au surface gives fertile ground for accelerating surface oxidation.[31] Unlike reactive $O_3$ molecules, $H_2O$ is a strongly bonded molecule, and thus it needs higher energy photons rather than UV to be dissociated. According to Fig. 7, more and more Au–O complexes are formed via reaction with free O up to about 200–300 min of EUV exposure.

It can be seen clearly in Fig. 7 that the rate of Au–O formation process is linked with the rate of $H_2O$ signal reduction. The sharp increase in Au–O signal in the first

60 min of EUV exposure is directly connected to the free O generation by $H_2O$ dissociation as evidenced by the rapid reduction in $H_2O$ signal during this time. The reduction in Au–O signal at higher EUV exposure times can also be correlated to leveling off $H_2O$ signal intensity. As mentioned earlier, the binding energy of $H_2O$ molecules to metal surface is influenced by the surface concentration of contaminants such as carbon and it weakens the adsorption energy of water molecules on metal surfaces.[29] Figure 4 clearly showed that Au top surface was continuously covered by carbon atoms with increasing EUV irradiation time. These observations also support our conclusion about the role of $H_2O$ dissociation under EUV exposure that causes Au oxidation.

Comparing Figs. 4, 6 and 7, one can explain the observed decrease in Au–O as a combination of two phenomena occurring simultaneously: (1) The instability of the Au–O bonds in the presence of more reactive elements/compounds[33] such as C and CO, which is due to the catalyzing behavior of Au (Refs. 31, 33, and 34) and (2) the gradual decrease in free O production rate by EUV induced $H_2O$ dissociation (as discussed previously) that suppresses further Au–O formation. We believe that the oxidation and reduction processes were in dynamic equilibrium during EUV exposure. Hence, the oxidation reaction was dominant when the free O production rate was high due to the $H_2O$ dissociation process.[29] On the other hand, when the $H_2O$ dissociation process was significantly reduced and the production of free oxygen atoms was suppressed, the Au–O reduction process surpasses Au oxidation in the presence of increasing carbon coverage (Fig. 4).

Finally, in order to confirm the role of EUV in Au surface chemical modification, another set of XPS scans for another Au sample was taken in a similar atmosphere without EUV radiation (Fig. 8). It was found clearly that the total carbon signal reached a saturation level on the top of the Au surface in about 1–2 h after stopping the sputter cleaning process. This observation confirms our previous conclusion about the hydrocarbons adsorption in the first 60 min of EUV
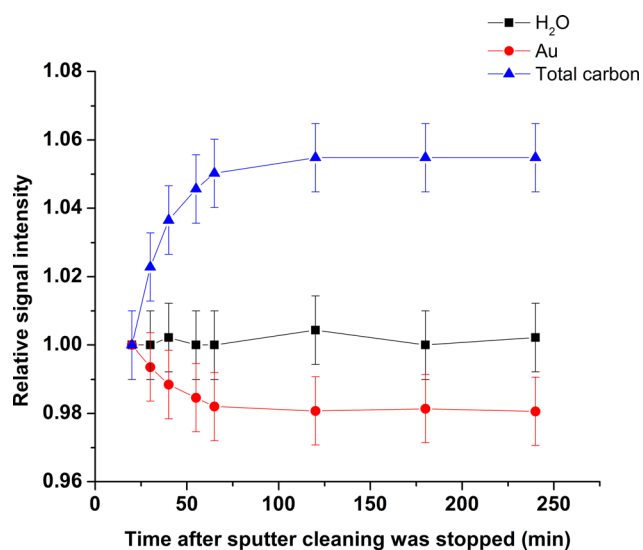


FIG. 8. (Color online) Temporal evolution of relative surface concentration of C, $H_2O$, and Au on the top of the Au surface in the absence of EUV radiation where the time is considered after stopping the sputter cleaning.

irradiation. Moreover, water concentration was found to be unchanged, and that strongly supports the suggestion about the relation between the reduction in surface water concentration and the EUV-induced dissociation and contamination processes that occur during EUV irradiation. On the other hand, in the absence of EUV radiation Au signal reached an equilibrium state in about 1 h, which occurs after an initial reduction due to surface coverage due to adsorption of contaminants (Fig. 8).

## IV. CONCLUSIONS

We report changes in surface chemistry, especially contamination processes of an Au surface in a high-vacuum atmosphere during EUV exposure. The changes in surface properties were monitored by recording high resolution XPS spectra of O 1$s$, C 1$s$, and Au 4$f$ regions. The total carbon (C 1$s$) peak area intensity was found to be increased by about 14% during the 9 h of EUV exposure. Careful XPS analysis of C 1$s$ edge reveals that C–H peak intensity increases with a higher rate in the first 60 min of EUV radiation, followed by the attainment of an equilibrium condition up to the end of the experiment. This behavior was explained in terms of accumulation of carbon in the form of hydrocarbons. The C–C line intensity was, however, increased with relatively lower rate compare to C–H in the first 60 min of EUV irradiation, but it was found to be increased linearly at a lower rate in the later time. The linear increase in C–C peak intensity after 60 min has been explained in light of an accumulation of graphitic carbon on Au due to EUV-assisted dissociation of adsorbed hydrocarbons.

Further analysis of the Au 4$f$ region revealed the formation of Au–O, which increased continuously as a function of EUV exposure until it arrived to its maximum within 200 and 300 min. The observed variation in Au–O peak intensity was again confirmed by analyzing the O 1$s$ region. Based on the XPS results, we can therefore conclude that sputter cleaned Au surface can be oxidized during EUV radiation in the presence of residual water molecules in a high-vacuum chamber, where the free O atoms originated via EUV-induced dissociation of water molecules. However, the reduction of the Au–O bonds becomes dominant above 200 min of EUV exposure due to a shortage in free O atoms, and the accumulation of reactive species (such as carbon and carbon-related species) with increasing EUV exposure.

## ACKNOWLEDGMENT

[1]J. Hollenshead and L. Klebanoff, J. Vac. Sci. Technol. B **24**, 64 (2006).
[2]K. Boller, R. P. Haelbich, H. Hogrefe, W. Jark, and C. Kunz, Nucl. Instrum. Methods Phys. Res. **208**, 273 (1983).
[3]N. Koster *et al.*, Microelectron. Eng. **61–62**, 65 (2002).
[4]W. M. Lytle, R. E. Lofgren, V. Surla, M. J. Neumann, and D. N. Ruzic, Proc. SPIE **7636**, 76360 (2010).
[5]K. Koida and M. Niibe, Appl. Surf. Sci. **256**, 1171 (2009).
[6]M. Yang, X. Tong, Y. Sun, D. Jiang, C. Zhou, and D. Zhang, Rev. Sci. Instrum. **80**, 033105 (2009).
[7]J. V. Hermans, D. Laidler, P. Foubert, K. D'Have, S. Cheng, M. Dusa, and E. Hendrickx, Proc. SPIE **8322**, 832202 (2012).
[8]C. Wagner *et al.*, Proc. SPIE **7969**, 79691F (2011).
[9]B. Wu and A. Kumar, J. Vac. Sci. Technol. B **25**, 1743 (2007).
[10]S. Braun, H. Mai, M. Moss, R. Scholz, and A. Leson, Jpn. J. Appl. Phys., Part 1 **41**, 4074 (2002).
[11]S. A. Bajt *et al.*, J. Microlithogr., Microfabr., Microsyst. **5**, 023004 (2006).
[12]L. Belau, J. Y. Park, T. Liang, H. Seo, and G. A. Somorjai, J. Vac. Sci. Technol. B **27**, 1919 (2009).
[13]N. B. Koster, J. C. J. van der Donck, J. K. Stortelder, A. J. de Jong, and F. T. Molkenboer, Proc. SPIE **8322**, 83220R (2012).
[14]K. Murakami *et al.*, Proc. SPIE **8322**, 832215 (2012).
[15]E. Louis, A. E. Yakshin, T. Tsarfati, and F. Bijkerk, Prog. Surf. Sci. **86**, 255 (2011).
[16]A. Al-Ajlony, A. Kanjilal, M. Catalfano, M. Fields, S. S. Harilal, A. Hassanein, and B. Rice, J. Vac. Sci. Technol. B **30**, 021601 (2012).
[17]G. Kyriakou, D. J. Davis, R. B. Grant, D. J. Watson, A. Keen, M. S. Tikhov, and R. M. Lambert, J. Phys. Chem. C **111**, 4491 (2007).
[18]J. F. Moulder, W. F. Stickle, P. E. Sobol, and K. D. Bomben, *Handbook of X-ray Photoelectron Spectroscopy* (Perkin-Elmer Corp., Eden Prairie, MN, 1992).
[19]J. R. Vig and J. W. L. Bus, IEEE Trans. Parts Hybrids Packag. **12**, 365 (1976).
[20]D. E. King, J. Vac. Sci. Technol. A **13**, 1247 (1995).
[21]S. Bajt, N. V. Edwards, and T. E. Madey, Surf. Sci. Rep. **63**, 73 (2008).
[22]J. P. Allain, M. Nieto, M. R. Hendricks, P. Plotkin, S. S. Harilal, and A. Hassanein, Rev. Sci. Instrum. **78**, 113105 (2007).
[23]A. Kanjilal, M. Catalfano, S. S. Harilal, A. Hassanein, and B. Rice, J. Appl. Phys. **111**, 063518 (2012).
[24]A. Egbert *et al.*, J. Microlithogr., Microfabr., Microsyst. **2**, 136 (2003).
[25]Z. Yue, W. Jiang, L. Wang, S. Gardner, and C. Pittmanjr, Carbon **37**, 1785 (1999).
[26]A. Nikitin, H. Ogasawara, D. Mann, R. Denecke, Z. Zhang, H. Dai, K. Cho, and A. Nilsson, Phys. Rev. Lett. **95**, 225507 (2005).
[27]A. I. Stadnichenko, S. V. Koshcheev, and A. I. Boronin, Moscow Univ. Chem. Bull. [Engl. Transl.] **62**, 343 (2007).
[28]T. Ishida, S. Tsuneda, N. Nishida, M. Hara, H. Sasabe, and W. Knoll, Langmuir **13**, 4638 (1997).
[29]T. Madey, N. Faradzhev, B. Yakshinskiy, and N. Edwards, Appl. Surf. Sci. **253**, 1691 (2006).
[30]M. Landmann, E. Rauls, and W. G. Schmidt, Phys. Rev. B **79**, 045412 (2009).
[31]B. Yoon, H. Hakkinen, and U. Landman, J. Phys. Chem. A **107**, 4066 (2003).
[32]W. Huang, H.-J. Zhai, and L.-S. Wang, J. Am. Chem. Soc. **132**, 4344 (2010).
[33]M. Gsior, B. Grzybowska, K. Samson, M. Ruszel, and J. Haber, Catal. Today **91–92**, 131 (2004).
[34]R. J. Madix and C. M. Friend, Nature (London) **479**, 482 (2011).